Global topology from an embedding

Robert Gilmore[1,2]**, Christophe Letellier**[2] **and Nicola Romanazzi**[1]

[1] Physics Department, Drexel University, Philadelphia, PA 19104, USA
[2] CORIA UMR 6614—Université de Rouen, Av de l'Université, BP 12,
F-76801 Saint-Etienne du Rouvray cedex, France

Abstract
An embedding of chaotic data into a suitable phase space creates a
diffeomorphism of the original attractor with the reconstructed attractor.
Although diffeomorphic, the original and reconstructed attractors may not be
topologically equivalent. In a previous work, we showed how the original and
reconstructed attractors can differ when the original is three-dimensional and of
genus-one type. In the present work, we extend this result to three-dimensional
attractors of arbitrary genus. This result describes symmetries exhibited by the
Lorenz attractor and its reconstructions.

PACS number: 05.45.−a

1. Introduction

Mappings of scalar and vector time series into suitable phase spaces are regularly used to
visualize processes that generate experimental data [1, 2]. When the mapping is an embedding,
a diffeomorphism exists between the original (experimental) attractor and the reconstructed
attractor. It is known from numerous examples that a single time series can be embedded in
different ways, giving rise to reconstructed attractors that 'look different'. We illustrate this
idea in figure 1, which shows two representations of the Lorenz attractor [3]. Under the usual
vector embedding $(x(t), y(t), z(t)) \rightarrow \mathbb{R}^3$, the attractor exhibits rotation symmetry about the
z-axis. The branched manifold [4–7] describing this representation of the Lorenz attractor is
shown in figure 1(a). It has a two-fold rotation symmetry about an axis through the origin
and perpendicular to the plane. On the other hand, under the scalar differential embedding
$(x(t), \dot{x}(t), \ddot{x}(t)) \rightarrow \mathbb{R}^3$ the reconstructed attractor exhibits inversion symmetry through the
origin [6–9]. The branched manifold describing this reconstruction of the Lorenz attractor is
shown in figure 1(b), where inversion symmetry is clearly exhibited. These two representations
of the Lorenz attractor look different: in fact they are topologically inequivalent in the sense
that there is no smooth deformation of phase space that transforms one into the other. There
is no family of smooth nonsingular transformations in $\mathbb{R}^3$ that deforms an object with rotation

(a)

(b)
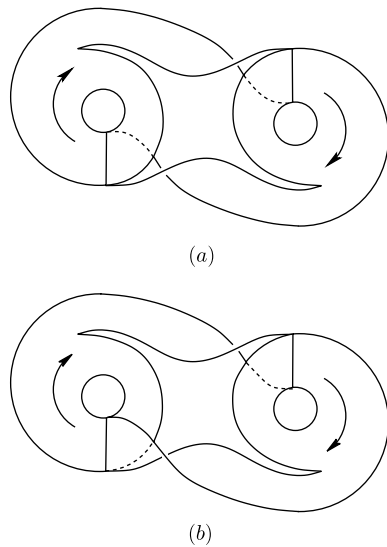
Figure 1. Branched manifolds describing two representations of the Lorenz attractor: (*a*) with rotation symmetry; (*b*) with inversion symmetry. The two attractors are related by a diffeomorphism restricted to the attracting set but they are not topologically equivalent.

symmetry to the one with inversion symmetry. The two representations of this attractor are diffeomorphic but topologically inequivalent.

The problem can be presented more precisely as follows. An experimental attractor can be reconstructed (recreated, represented) by an embedding. An embedding is a diffeomorphism between the original and the reconstructed attractor. Two different embeddings create topologically equivalent attractors if there is an isotopy that takes one diffeomorphism into the other [10]: that is, the two diffeomorphisms are both members of a smooth one-parameter family of diffeomorphisms. The central point is that not every pair of diffeomorphisms can be joined by a smooth isotopy [10]. When two diffeomorphisms are not isotopic, the attractors they recreate are not topologically equivalent [6, 7, 11]. It is known that diffeomorphic but topologically inequivalent embeddings can result from time delay embeddings with different delays [11].

This raises an important question. How much of what we learn by studying a reconstructed attractor depends on the embedding and how much is independent of the embedding? The properties that are independent of the embedding characterize the original attractor.

Geometric properties, such as the spectrum of fractal dimensions, are in principle diffeomorphism independent [12] (but see [13]). Dynamical properties, such as the spectrum of Lyapunov exponents, are also diffeomorphism independent (but see [14, 15]). As a result, these real numbers can usually be assumed to be valid for the original attractor when computed from any reconstructed attractor. Conversely, they cannot be used to distinguish one embedding from another. Nor do these real numbers shed any light on the *mechanism* generating chaotic behavior [16].

Topological indices shed a great deal of light on the mechanism generating chaotic behavior [6, 7, 17]. At the same time they are not embedding invariants. As a result, we must understand what part of the topological information obtained from a reconstructed attractor is independent of the embedding, and what part is not. This program has been completed for three-dimensional attractors that are contained in a bounding torus of genus one [16]. In this

case, we find that embeddings have three degrees of freedom: parity, global torsion and knot type.

In the present work, we extend these results to three-dimensional attractors of higher genus ($g > 1$). These include many attractors generated by autonomous dynamical systems with two-fold or higher-fold symmetry [7, 18–20]. We find the analogs of parity and global torsion, but do not discuss knot type. All embeddings reveal the same stretching and folding mechanism.

Our work is restricted to three-dimensional attractors. These are attractors that exist in a three-dimensional manifold, not necessarily $\mathbb{R}^3$. This restriction is necessary because the topological indices that we compute (linking numbers, relative rotation rates) are for closed periodic orbits that have a rigid organization in three-dimensional manifolds but not in higher dimensional manifolds [10, 17].

In section 2, we briefly review the results for the genus-one case. In section 3, we construct the analog, in the higher-genus case, for global torsion in the genus-one case. In section 4, we construct the analog, in the higher-genus case, of parity in the genus-one case. We discuss the implications of our results in section 5.

2. Review of genus-one results

In [16] we assumed that an experimental attractor is contained in a three-dimensional manifold that has the global topology of a genus-one torus. An embedding constructs a diffeomorphism between the original and reconstructed attractors. A different embedding provides another diffeomorphism between the original and another reconstructed attractor. The two (in fact, all) reconstructed attractors are diffeomorphic when restricted to the attracting set. The question of how embeddings of an unseen attractor can differ simplifies to the question of how diffeomorphisms of a torus to a torus can differ.

Diffeomorphisms form a group. The subset of diffeomorphisms that is isotopic to the identity forms an invariant subgroup [10, 16]. In fact, this invariant subgroup cannot change any topological indices, which are integers or rational fractions [6, 17]. The quotient group, diffeomorphisms/(diffeomorphisms isotopic to identity), is discrete and describes the equivalence classes of diffeomorphisms of the torus [10, 16]. Each element in this discrete group changes the topological indices in a different way.

The action of this discrete group can be understood by its action on the boundary of the torus [10, 16]. This is done as follows. Cut the torus open and stretch it out along the central axis. Label the position along the axis by an angle ϕ, $0 \leqslant \phi \leqslant 2\pi$. Choose a plane at ϕ and rotate the intersection of the torus boundary with this plane by an angle θ. Set $\theta(\phi = 0) = 0$. Now close the torus backup. A diffeomorphism is created by this process only when periodic boundary conditions are satisfied, so that $\theta(\phi = 2\pi) = 2\pi n$, with n an integer [21]. This integer is the degree of freedom called global torsion [6, 16, 22].

A parity transformation is obtained by reflecting the torus in an external mirror. Parity is a single index: $P = \pm 1$.

A genus-one torus can be embedded into $\mathbb{R}^3$ by allowing its central axis to follow the curve of any knot. We do not yet know how to classify knots algebraically. Even less is known about extrinsic embeddings of higher-genus tori in $\mathbb{R}^3$. We do not discuss extrinsic embeddings of genus-g tori ($g > 1$) into $\mathbb{R}^3$ in the present work.

3. Analog of global torsion

A bounding torus of genus g [23, 24] can be constructed, Lego© fashion, from Y-junctions. These are two-dimensional manifolds with three ports. For our purposes there are two types:
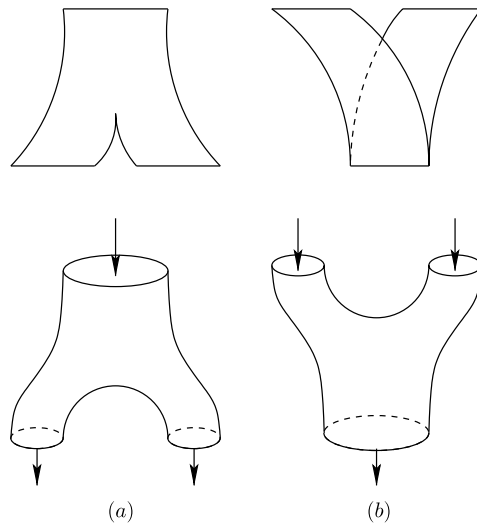
Figure 2. Bounding tori can be constructed from two types of units with three ports. (*a*) Splitting units have one input port and two output ports; (*b*) joining units have two input ports and one output port.

splitting units with one input port and two output ports and joining units with two input ports and one output port. These units are shown in figures 2(*a*) and (*b*). A canonical bounding torus of genus three is shown in figure 3. The Lorenz attractor is contained in a bounding torus of this type. The figure shows how this bounding torus is decomposed into two input units and two output units. As usual, output ports connect to input ports, and there are no free ends [4–6, 17].

In figure 3(*b*), we insert a 'flow tube' between each output port and the input port on a different unit that it is connected to. Periodic boundary conditions are satisfied if each of these tubes is rotated through an integer number of full twists [16, 21]. Since there are $4 = 2(3 - 1)$ units in the decomposition of the genus-three torus, each has three ports, and one tube is inserted between each pair of ports, there is a total of $(3 - 1) \times 3$ tubes, each of which can exhibit an integer twist. Each configuration is diffeomorphic but not isotopic to every other.

The general result is that a genus-g torus can be decomposed into $g - 1$ splitting units and $g - 1$ joining units, so that $2(g - 1) \times (3/2) = 3(g - 1)$ tubes can be inserted. As a result, the genus-g analog of the genus-one global torsion is an index Z^N, $N = 3(g - 1)$. This is a set of $N = 3(g - 1)$ integers, one for each inserted flow tube. Recall that for bounding tori, $g = 1$ or $g \geqslant 3$ [23, 24].
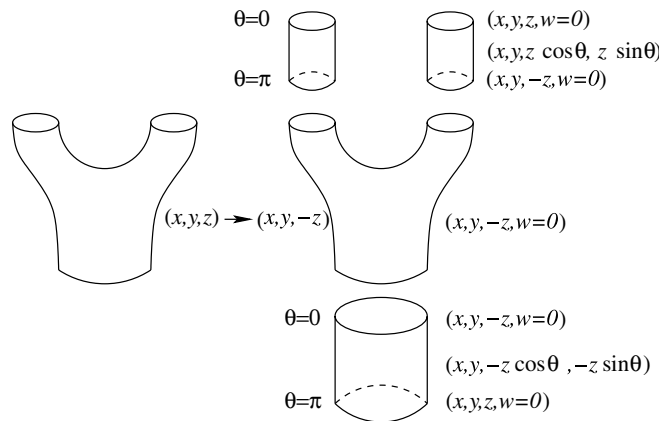
4. Local reflections

The genus-g analog of the parity transformation in the genus-one case consists of local reflections.

The construction of local reflections is subtle. It is clear what a local reflection does to a branched manifold that describes a genus-g flow. It simply maps a joining unit of a branched manifold into its mirror image. This is illustrated in figure 1. The problem is that local reflections in $\mathbb{R}^3$ cannot be used in general to create diffeomorphisms between the two flows responsible for the branched manifolds related by a local reflection, as shown in figure 1. The exception occurs when a symmetry is involved [7].
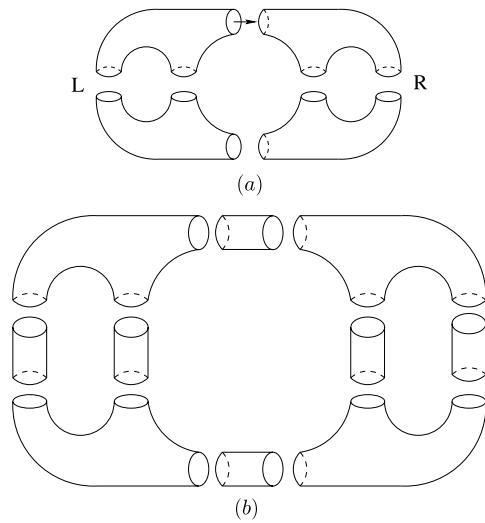
Figure 3. (*a*) A genus-three bounding torus is decomposed into two splitting units and two joining units. (*b*) Each input/output port pair is separated by a cylindrical flow tube. Periodic boundary conditions are satisfied if each flow tube is given an integer twist. There are six flow tubes, so the analog of global torsion in the genus-three case is Z^6. In the genus-g case, the analog is $Z^{3(g-1)}$.

Figure 4. Three flow tubes are attached to a joining unit. The flow in the joining unit undergoing local reflection is immersed in $\mathbb{R}^4$ according to $(x, y, z) \rightarrow (x, y, -z, w = 0)$. The flow in the flow tubes is rotated in the (z, w) plane according to $(z, w) \rightarrow (z \cos \theta - w \sin \theta, z \sin \theta + w \cos \theta)$, where $\theta = 0$ at the entrance of each added flow tube and $\theta = \pi$ at the exit. This creates a diffeomorphism between the original flow in $\mathbb{R}^3 \subset \mathbb{R}^4$ and a nonisotopic flow in a three-dimensional manifold $M^3 \subset \mathbb{R}^4$.

We can create diffeomorphisms that include local reflections as shown in figure 4. Choose a joining unit and insert a flow tube of length L at each port. Each flow tube contains a branch of the branched mainfold describing the attractor generated by the flow. Deform the flow so that it is 'laminar' or 'uniform' in each flow tube. By 'laminar' or 'uniform', we mean the flow assumes the form $\dot{x} = \text{const}, \dot{y} = 0, \dot{z} = 0$ in local coordinates. Here, x is a coordinate along the central axis of the cylindrical flow tube, y is a coordinate in the plane of the branch

through the flow tube and z measures the distance above or below this plane. The branch occurs in the plane $z = 0$.

Now embed the three-dimensional flow into $\mathbb{R}^4$ by introducing a fourth coordinate, w. The original three-dimensional flow has coordinates $(x(t), y(t), z(t), w)$ with $w = 0$. Now create a diffeomorphism between this flow in a three-dimensional manifold in $\mathbb{R}^4$, $\mathbb{R}^3 \subset \mathbb{R}^4$, and another three-dimensional manifold in $\mathbb{R}^4$, $M^3 \subset \mathbb{R}^4$, as follows. Perform a rotation through π radians in the z, w plane in each flow tube according to $(z, 0) \rightarrow (z \cos(x/L), z \sin(x/L))$. This rotation maps coordinate (y, z) at the input side of a flow tube ($x = 0$) to coordinate $(y, -z)$ at the output side ($x = L$). In the joining unit, map coordinates (x, y, z) to their mirror images $(x, y, -z)$ in the $z = 0$ plane. This set of transformations creates a diffeomorphism between flows in $\mathbb{R}^3$ and M^3. The projection of the branched manifold describing the flow in M^3 into $\mathbb{R}^3$ differs from the branched manifold describing the flow in $\mathbb{R}^3$ by the mirror image of the joining unit, as shown in figure 1. The two branched manifolds are 1-1, locally isomorphic, and not isotopic (i.e., globally distinct). The flows in $\mathbb{R}^3$ and M^3 are diffeomorphic but the projection of the flow in $M^3 \subset \mathbb{R}^4$ into $\mathbb{R}^3$ is not an embedding. This phenomenon has already been encountered in descriptions of autonomous-coupled dynamo systems [25].

Local reflections can be carried out independently on each of the $g - 1$ joining units. The effect of a local reflection can be seen by comparing the two representations of the Lorenz flow shown in figure 1. A local reflection has been carried out on a joining unit in figure 1(b). This operation transforms a rotation-symmetric representation of the attractor (figure 1(a)) to an inversion-symmetric representation of the attractor (figure 1(b)). We can describe the two representations shown in figure 1 as (+, +) and (−, +), with the positions referring to the joining units on the left and right, and the signs referring to a reflection (−) or no reflection (+). Two other representations are easily constructed with signatures (−, −) and (+, −). The latter two are related to the former two by a global reflection transformation.

A strange attractor in a genus-g torus has $2^{(g−1)}$ representations related by local reflections. They are all related to each other by diffeomorphisms acting in $\mathbb{R}^4$. None is isotopic to any other.

5. Summary

Embeddings based on scalar or vector time series create diffeomorphisms between the original attractor and the reconstructed attractor. Different embeddings create diffeomorphic reconstructed attractors that are not necessarily topologically equivalent, that is, not isotopic. Since topology indicates clearly what are the mechanisms (stretching, folding, tearing, squeezing) that generate complex behavior [17], it is an important question to ask: How much do we learn about the original attractor by carrying out a topological analysis of a reconstructed attractor, and how much about the embedding do we learn? For the genus-one case, the result is that embeddings can differ by three degrees of freedom: parity, global torsion and knot type. The mechanism displayed is independent of the embedding [16].

In this work, we have answered this question for attractors contained in higher-genus bounding tori. We have done this by constructing a discrete classification of all nonisotopic (topologically inequivalent) diffeomorphisms of a bounding torus into itself. We have enumerated the degrees of freedom, not including how the bounding torus can be embedded into $\mathbb{R}^3$. There are two degrees of freedom: local torsion in each of $3(g - 1)$ flow tubes and local reflections in each of $g - 1$ joining units. It is useful to regard these degrees of freedom as follows: there are $2^{(g−1)}$ topologically inequivalent representations of an attractor related to each other by different subsets of local reflection transformations. Each is the patriarch

for a $3(g-1)$-parameter family of strange attractors defined by an index $Z^{3(g-1)}$ [21]. All representations are topologically inequivalent.

What is an invariant of an embedding, and the same for each of the $2^{(g-1)} \otimes Z^{3(g-1)}$ representatives of a strange attractor is the mechanism that generates the dynamics. The mechanism describes how the flow is split apart to flow to different regions of the phase space, and how different parts of the phase space are joined [6, 16]. This information is encoded in the transition matrix: stretching is described by the rows of this matrix and squeezing by the columns of this matrix [23, 24].

Acknowledgment

References

[1] Packard N H, Crutchfield J P, Farmer J D and Shaw R S 1980 *Phys. Rev. Lett.* **45** 712
[2] Takens F 1981 *Detecting Strange Attractors in Turbulence (Lecture Notes in Mathematics* vol 898*)* ed D A Rand and L-S Young (New York: Springer) pp 366-81
[3] Lorenz E N 1963 *J. Atmos. Sci.* **63** 130
[4] Birman J S and Williams R F 1983 *Topology* **22** 47
[5] Birman J and Williams R F 1983 *Cont. Math.* **20** 1
[6] Gilmore R and Lefranc M 2002 *The Topology of Chaos* (New York: Wiley)
[7] Gilmore R and Letellier C 2007 *The Symmetry of Chaos* (New York: Oxford)
[8] Letellier C and Gouesbet G 1996 *J. Phys. II* **6** 1615
[9] Letellier C, Gouesbet G and Rulkov N 1996 *Int. J. Bifurcation Chaos* **6** 2531
[10] Rolfsen D 1990 *Knots and Links* (Providence, RI: American Mathematical Society)
[11] Tsankov T D, Nishtala A and Gilmore R 2004 *Phys. Rev.* E **69** 056215 1–8
[12] Eckmann J P and Ruelle D 1985 *Rev. Mod. Phys.* **57** 617
[13] Lefranc M, Hennequin D and Glorieux P 1992 *Phys. Lett.* A **163** 269
[14] Brown R, Bryant P and Abarbanel H 1991 *Phys. Rev.* A **43** 2792
[15] Sauer T D, Tempkin J A and Yorke J A 1998 *Phys. Rev. Lett.* **81** 4341
[16] Romanazzi N, Lefranc M and Gilmore R 2007 *Phys. Rev.* E **75** 066214
[17] Gilmore R 1998 *Rev. Mod. Phys.* **70** 1455
[18] Miranda R and Stone E 1993 *Phys. Lett.* A **178** 105
[19] Letellier C and Gilmore R 2001 *Phys. Rev.* E **63** 016206
[20] Aziz-Alaoui M A 1999 *Int. J. Bifurcation Chaos* **9** 1009
[21] Gilmore R 2007 *Chaos* **17** 013104
[22] Solari H G and Gilmore R 1988 *Phys. Rev.* A **37** 3096
[23] Tsankov T D and Gilmore R 2003 *Phys. Rev. Lett.* **91** 134104
[24] Tsankov T D and Gilmore R 2004 *Phys. Rev.* E **69** 056206
[25] Moroz I M, Letellier C and Gilmore R 2007 *Phys. Rev.* E **75** 046201